Published in final edited form as:
Mol Cell. 2011 May 6; 42(3): 319–329. doi:10.1016/j.molcel.2011.03.019.

Regulation of DNA End Joining, Resection, and Immunoglobulin Class Switch Recombination by 53BP1

Anne Bothmer[1,4], **Davide F. Robbiani**[1,4], **Michela Di Virgilio**[1], **Samuel F. Bunting**[3], **Isaac A. Klein**[1], **Niklas Feldhahn**[1], **Jacqueline Barlow**[3], **Henry T. Chen**[3], **David Bosque**[1], **Elsa Callen**[3], **André Nussenzweig**[3,5], and **Michel C. Nussenzweig**[1,2,5]

[1] Laboratory of Molecular Immunology, The Rockefeller University, New York, New York 10065, United States

[2] Howard Hughes Medical Institute, The Rockefeller University, New York, New York 10065, United States

[3] Experimental Immunology Branch, National Cancer Institute, National Institutes of Health, Bethesda, Maryland 20892, United States

Summary

53BP1 is a DNA damage protein that forms phosphorylated H2AX (γ-H2AX) dependent foci in a 1 Mb region surrounding DNA double strand breaks (DSBs). In addition, 53BP1 promotes genomic stability by regulating the metabolism of DNA ends. We have compared the joining rates of paired DSBs separated by 1.2 kb to 27 Mb on chromosome 12 in the presence or absence of 53BP1. 53BP1 facilitates joining of intrachromosomal DSBs but only at distances corresponding to γ-H2AX spreading. In contrast, DNA end protection by 53BP1 is distance independent. Furthermore, analysis of 53BP1 mutants shows that chromatin association, oligomerization, and N-terminal ATM phosphorylation are all required for DNA end protection and joining as measured by immunoglobulin class switch recombination. The data elucidate the molecular events that are required for 53BP1 to maintain genomic stability and point to a model wherein 53BP1 and H2AX cooperate to repress resection of DSBs.

Introduction

53BP1 is a DNA damage response protein that rapidly forms nuclear foci in response to DNA damage (Anderson et al., 2001; Rappold et al., 2001; Schultz et al., 2000). This process is dependent on PIKK- (ATM/ATR/DNA-PKcs) induced phosphorylation of histone H2AX (γ-H2AX, (Celeste et al., 2003; Fernandez-Capetillo et al., 2002; Ward et al., 2003; Yuan and Chen, 2010)). γ-H2AX in turn recruits the E3 ubiquitin ligases RNF8 and RNF168 (Doil et al., 2009; Huen et al., 2007; Kolas et al., 2007; Mailand et al., 2007; Stewart et al., 2009) which promote histone ubiquitylation at sites of DSBs. The way in which ubiquitylation facilitates the accumulation of 53BP1 at sites of DSBs has not yet been defined; but one possible scenario is that ubiquitylation exposes constitutive chromatin

*correspondence: nussen@mail.rockefeller.edu, phone: (212) 327-8067 or nussenza@exchange.nih.gov, phone: (301) 435-6425.
4 and 5equal contribution

marks, such as H4K20^{me2}, to which 53BP1 then binds via its tandem tudor domain (Botuyan et al., 2006; Mailand et al., 2007).

In addition to its chromatin binding tudor domain, 53BP1 contains an oligomerization domain, tandem BRCA1 C-terminal (BRCT) domains, and numerous sites that can be modified post-translationally (Adams and Carpenter, 2006). Homo-oligomerization and interaction between the tudor domains and H4K20^{me2} are required for 53BP1 focus formation in response to DNA damage (Botuyan et al., 2006; Iwabuchi et al., 2003; Ward et al., 2006; Ward et al., 2003; Zgheib et al., 2009). In contrast, the C-terminal tandem BRCT domains are not essential for focus formation, but mediate the interaction between 53BP1 and EXPAND1, a protein shown to promote chromatin changes after DNA damage and to facilitate repair (Huen et al., 2010; Ward et al., 2006). Finally, the N-terminal portion of 53BP1 lacks defined structural domains but contains multiple S/T-Q motifs, which are phosphorylation targets of ATM. Although mutating these residues to alanine alters the kinetics of resolution of DNA damage foci, it does not affect the formation of 53BP1 foci in response to DNA damage (DiTullio et al., 2002; Morales et al., 2003; Ward et al., 2006).

In addition to DNA damage dependent focus formation, 53BP1 is required to protect DSBs from end resection (Bothmer et al., 2010; Bunting et al., 2010). The absence of 53BP1 facilitates resection, thereby relieving a block to homologous recombination in Brca1 mutant cells, promoting degradation of DNA ends during V(D)J recombination, and promoting microhomology-mediated alternative NHEJ (A-NHEJ) during immunoglobulin class switch recombination (CSR) (Bothmer et al., 2010; Bunting et al., 2010; Difilippantonio et al., 2008). CSR is a B cell specific antibody diversification reaction leading to the production of antibodies of different isotypes with altered effector functions (Manis et al., 2004; Ward et al., 2004). Mechanistically CSR is a deletional recombination reaction between paired DSBs in highly repetitive *Ig* switch regions (S-regions) separated by 60–200 kb (Stavnezer et al., 2008). Each S-region contains a characteristic repetitive sequence, which can also serve as a substrate for proximal microhomology-mediated intra-switch repair by A-NHEJ at the expense of CSR (Boboila et al., 2010a; Boboila et al., 2010b; Bothmer et al., 2010; Reina-San-Martin et al., 2007). Efficient rearrangements require synapsis and repair by classical-NHEJ (C-NHEJ). In addition to CSR, 53BP1 is also required for the joining of distal DSBs during V-J recombination at the TCRα locus (Difilippantonio et al., 2008), and for the fusion of de-protected telomeres (Dimitrova et al., 2008).

Several non-mutually exclusive models have been put forward to explain how 53BP1 helps maintain genome stability and contributes to CSR. One model proposes that 53BP1 facilitates distal DSB joining by synapsing paired DSBs, either by altering local chromatin structure or by increasing chromatin mobility (Difilippantonio et al., 2008; Dimitrova et al., 2008). 53BP1 may also favor CSR by protecting DSBs in Ig switch regions from resection, thereby limiting A-NHEJ mediated intra-switch recombination between homologous sequences while promoting productive inter-switch rearrangements by C-NHEJ (Bothmer et al., 2010).

Here we show that the effects of 53BP1 on joining depend on the distance between the broken ends while DNA end protection by 53BP1 is a distance independent function. We furthermore define the domains of 53BP1 that are required for CSR and DNA end protection.

Results

Role of distance in joining of DSBs

During CSR, activation induced cytidine deaminase (AID) produces tandem DSBs in Ig heavy chain (IgH) switch regions separated by 60–200 kb. 53BP1 is required for the efficient joining between IgH switch breaks, and similarly facilitates the joining of I-SceI induced DSBs separated by 96 kb (Bothmer et al., 2010). To determine how distance affects the joining efficiency of paired DSBs on the chromosome bearing the IgH locus, we produced additional knock-in mice bearing I-SceI sites separated by 1.2 kb or 27 Mb on chromosome 12 ($IgH^{I\text{-}1k}$ and $IgH^{I\text{-}27M}$ respectively, Figures S1A and S1D). $IgH^{I\text{-}1k}$ and $IgH^{I\text{-}27M}$ showed normal B cell development and CSR to IgG1 upon stimulation with LPS and IL4 (Figures S1B and S1E).

To compare the joining efficiency of DSBs at different distances on the same chromosome, we infected $IgH^{I\text{-}1k/+}AID^{-/-}$ and $IgH^{I\text{-}27M/+}AID^{-/-}$ B cells with an I-SceI expressing virus or an inactive I-SceI* control and measured recombination frequencies by sample dilution PCR (Figure S1C). Strikingly, the efficiency of joining DSBs separated by 27 Mb was >30 fold lower than that of DSBs separated by 1.2 kb (0.0048×10^{-2} versus 0.17×10^{-2}, $p<0.0001$, grey bars in Figures 1B and 1E) or 96 kb (0.7×10^{-2}, Bothmer et al., 2010). To determine how distal intrachromosomal repair compares with trans-chromosomal joining, we produced mice with paired I-SceI sites on chromosomes 12 and 15 (IgH^{I} and Myc^{I}, respectively; (Robbiani et al., 2008)) and generated translocations by infecting cells with I-SceI viruses. The joining frequency of I-SceI infected $IgH^{I/+}Myc^{I/+}AID^{-/-}$ B cells was 0.0027×10^{-2} per cell, which is comparable to the joining between I-SceI sites separated by 27 Mb in $IgH^{I\text{-}27M/+}AID^{-/-}$ (Figures 1E and 1H, grey bars). We conclude that the joining of proximal (1.2 or 96 kb) intra-chromosomal DSBs is significantly more efficient than distal (27 Mb) intra-chromosomal joining, and that the latter is similar to trans-chromosomal joining.

Loss of 53BP1 decreases the joining efficiency of I-SceI induced DSBs separated by 96 kb at the IgH locus, although the effect is less pronounced than for AID mediated CSR (Bothmer et al., 2010). To determine the role of 53BP1 in distal vs. proximal repair of paired DSBs, we compared joining between I-SceI sites in 53BP1 deficient $IgH^{I\text{-}1k}$ (proximal), $IgH^{I\text{-}27M}$ (distal) and $IgH^{I}Myc^{I}$ (interchromosomal) B cells ($IgH^{I\text{-}1k/+}AID^{-/-}53BP1^{-/-}$, $IgH^{I\text{-}27M/+}AID^{-/-}53BP1^{-/-}$ and $Myc^{I/+}IgH^{I/+}AID^{-/-}53BP1^{-/-}$ B cells, respectively). In contrast to the joining of DSBs separated by 96 kb (Bothmer et al., 2010), the absence of 53BP1 did not reduce the frequency of joining between I-SceI sites separated by 1.2 kb or 27 Mb on the same chromosome or sites on different chromosomes. (Figures 1B, 1E, 1H and S1F, S1G, S1H). We conclude that in contrast to facilitating the joining of DSBs separated by 96 kb, the loss of 53BP1 does not alter the joining frequency of more proximal or distal DSBs.

The loss of 53BP1 results in increased DNA end-resection (Bothmer et al., 2010). To determine whether this effect is dependent on distance, we measured end resection in $IgH^{I\text{-}1k/+}AID^{-/-}53BP1^{-/-}$ and $IgH^{I\text{-}27M/+}AID^{-/-}53BP1^{-/-}$ B cells and the respective 53BP1 proficient controls. Joins with deletions of more than 35 nts (indicative of extensive end-processing) increased from 37.2 % in $IgH^{I\text{-}1k/+}AID^{-/-}$ to 52.4 % in $IgH^{I\text{-}1k/+}AID^{-/-}53BP1^{-/-}$ and from 55.5 % in $IgH^{I\text{-}27M/+}AID^{-/-}$ to 75.5 % in $IgH^{I\text{-}27M/+}AID^{-/-}53BP1^{-/-}$ (Figures 1C and 1F). We conclude that 53BP1's ability to prevent end resection is independent of distance between paired DSBs.

In summary, 53BP1 has a distance independent function in the prevention of DNA end resection, and a distance dependent function in facilitating the joining of DSBs.

BRCT domains

To investigate the function of the BRCT domains of 53BP1 in CSR, we deleted the region corresponding to amino acids 1708–1969 from the mouse germline ($53BP1^{\Delta BRCT}$; Figures 2A and S2A). Lymphocyte development and CSR were normal in $53BP1^{\Delta BRCT}$ mice, despite lower than wild type levels of the mutant protein (Figures 2B, 2C and S2B).

To determine whether the BRCT domains are required for DSB end protection, we produced $53BP1^{\Delta BRCT/-}IgH^{I\text{-}96k/+}$ mice and assayed the resection of paired I-SceI breaks. We found a minor increase in DNA end resection compared to controls, which is probably due to the decreased expression level of the mutant protein (Figures 2B and 2D). We conclude that the BRCT domains of 53BP1 are dispensable for CSR and the protection of DNA ends from resection.

53BP1 chromatin association

53BP1 binds to $H4K20^{me2}$, a constitutive histone modification, and forms nuclear foci in response to DNA damage (Botuyan et al., 2006; Schultz et al., 2000). To determine whether 53BP1 is chromatin-associated in B cells, we fractionated unstimulated B cells before or after treatment with ionizing radiation (IR). We found that a portion of the total cellular 53BP1 is chromatin associated in the steady state even in the absence of DNA damage (Figure 3A). This is consistent with the finding that 53BP1 constitutively associates with chromatin in a manner independent of RNF8 (Santos et al., 2010). Furthermore, chromatin association did not increase significantly after irradiation.

Residue D1521 in the tudor domain of 53BP1 is required for binding to $H4K20^{me2}$ (Botuyan et al., 2006). To test the role of this interaction in CSR and DNA resection, we produced D1518R mutant mice ($53BP1^{DR}$) bearing a single amino acid substitution that is equivalent to D1521R in humans (Figure 3B and S3A). Lymphocyte development was similar to wild type in $53BP1^{DR}$ mice (Figure S3B), and the mutant $53BP1^{DR}$ protein was normally phosphorylated at Ser^{25} upon IR (Figure S3C). In agreement with previous studies, $53BP1^{DR}$ failed to form IR-induced foci and showed only faint accumulation at sites of laser scissor damage in mouse embryonic fibroblasts (MEFs; Figures 3C and S3D (Botuyan et al., 2006; Huyen et al., 2004)). In addition, $53BP1^{DR}$ was not chromatin associated in B cells (Figure 3D). We conclude that 53BP1 binds to chromatin constitutively through residue D1518 and that chromatin association is not required for 53BP1 phosphorylation.

To determine whether chromatin association is required for CSR, we stimulated $53BP1^{DR}$ B cells *in vitro*. Mutant B cells switched at about 10% of wild type levels, phenocopying $53BP1^{-/-}$ (Figure 3E). Loss of chromatin association also resulted in an increase in DNA end resection in $53BP1^{DR}IgH^{I\text{-}96k/+}$ comparable to $53BP1^{-/-}IgH^{I\text{-}96k/+}$ controls (Figure 3F). We conclude that 53BP1 is constitutively chromatin associated and that this association is required for CSR and for the protection of DNA ends from resection.

H2AX is required for stable 53BP1 DNA damage focus formation, and its deficiency impairs CSR, but to a lesser extent than absence of 53BP1 (Celeste et al., 2002; Fernandez-Capetillo et al., 2002; Reina-San-Martin et al., 2003). Moreover, 53BP1 was reported to interact with H2AX (Ward et al., 2003). To determine if the chromatin association of 53BP1 depends on this histone variant, we assayed H2AX deficient B cells. Although H2AX is required for 53BP1 foci, we found that H2AX is dispensable for 53BP1 chromatin association (Figure 4A). To determine if H2AX is required to prevent DNA resection, we assayed $IgH^{I\text{-}96k/+}AID^{-/-}$ $H2AX^{-/-}$ B cells. We found that resection was increased in the absence of H2AX to levels comparable to $53BP1^{-/-}$ (51.7 % compared to 35.8 % in $IgH^{I\text{-}96k}AID^{-/-}$ control, Figure 4B). Interestingly, while allowing for resection, absence of H2AX does not reverse radial fusions that are observed in PARP inhibitor (KU58948)

treated Brca1 mutant cells (Figure 4C). Thus, although 53BP1 can be constitutively chromatin associated in the absence of H2AX, this alone is not sufficient to prevent the extensive resection.

The oligomerization domain of 53BP1 is required for CSR

The central region of 53BP1 is required for 53BP1 oligomerization (Ward et al., 2006; Zgheib et al., 2009) and contains residues that are phosphorylated by ATM (S1219; (Lee et al., 2009)), ubiquitilated by Rad18 (K1268; (Watanabe et al., 2009)), and methylated by PRMT1 (R1398, R1400, R1401; (Boisvert et al., 2005)). To determine the role of this region *in vivo*, we produced mice that express a mutant form of 53BP1 lacking this region (Figures 5A and S4A). $53BP1^{\Delta 1210–1447}$ protein was expressed at normal levels, and lymphocyte development in $53BP1^{\Delta 1210–1447}$ mice was similar to wild type (Figures S4B and S4C).

However, $53BP1^{\Delta 1210–1447}$ B cells are similar to null mutant cells in CSR (Figure 5B). To confirm this result and identify the responsible activity, we produced four region-specific mutant retroviruses and assayed them for their ability to rescue IgG1 switching in $53BP1^{-/-}$ B cells (Figure 5C, 5D and S4D; since full-length 53BP1 cannot be expressed by retroviruses, deletion of the BRCT domain, which is similar to wild type (see Figure 2) can be used for retroviral expression). $53BP1^{\Delta 1231–1270}$, which lacks the oligomerization domain, was the only mutant that failed to rescue CSR, despite partially retaining the ability to bind chromatin (Figure 5D and 5E (Zgheib et al., 2009)). We conclude that the oligomerization domain in 53BP1 is required for class switch recombination but that residues S1219, K1268 and R1398/R1400/R1401 are not.

Residues 1052 to 1710 of 53BP1 include the tudor and oligomerization domains, which are sufficient for chromatin binding and DNA damage focus formation (Figure 5F and (Ward et al., 2003; Zgheib et al., 2009)). However, retrovirally expressed $53BP1^{1052–1710}$ was unable to rescue CSR (Figure 5G and S4E). We conclude that chromatin binding, oligomerization, and focus formation are insufficient to promote CSR, suggesting that the N-terminus of 53BP1 may play an important role in this reaction.

Phosphorylation sites at the N-terminus of 53BP1

To examine the role of the N-terminus of 53BP1 in CSR, we produced and tested additional mutants, including: (1) smaller N-terminal deletions ($53BP1^{901–1710}$ and $53BP1^{459–1710}$), (2) internal deletions corresponding to the amino acids encoded by exons 3–12 ($53BP1^{\Delta 61–901}$), 7–12 ($53BP1^{\Delta 216–901}$), and 12 alone ($53BP1^{\Delta 459–901}$), and (3) alanine substitution mutants of S/T-Q consensus sites for ATM phosphorylation ($53BP1^{8A}$, $53BP1^{7A}$, $53BP1^{15A}$, $53BP1^{28A}$; (Morales et al., 2003; Ward et al., 2006)). We found that all of the deletion mutants were unable to rescue CSR (Figure S5A and S5B). The alanine substitution mutants $53BP1^{8A}$, $53BP1^{7A}$, $53BP1^{15A}$, $53BP1^{28A}$, displayed a phenotype that correlated with the number of substitutions. $53BP1^{8A}$ showed 90% of WT CSR whereas $53BP1^{28A}$ was similar to the null mutant (Figure 6A, 6B and S5C). Despite its inability to rescue CSR, $53BP1^{28A}$ bound to chromatin and formed IR-foci (Figure 6C and 6D). We conclude that multiple S/T-Q target sites for ATM phosphorylation at the N-terminus of 53BP1 are required for CSR.

The oligomerization domain and N-terminal phosphorylation sites in 53BP1 protect DNA ends from processing

Loss of 53BP1 rescues homologous recombination in Brca1 mutant cells by facilitating the processing of DNA ends (Bunting et al., 2010). To determine which domains of 53BP1 are required for DNA end protection in Brca1 mutant cells, we infected $Brca1^{\Delta 11/\Delta 11}53BP1^{-/-}$ B cells with 53BP1 mutant retroviruses and measured the frequency of radial chromosome

structures upon treatment with the PARP inhibitor (Bunting et al., 2010). Whereas 12 radial structures were found among 100 metaphases in Brca1$^{\Delta 11/\Delta 11}$53BP1$^{-/-}$ B cells infected with a negative control virus, 54 were present upon infection with 53BP1$^{1–1710}$ (average of two independent experiments, Figure 7A and S6A). Confirming our previous finding with 53BP1^{DR} B cells, showing that chromatin binding is required for protection from DNA resection, a 53BP1^{D1521R} virus did not rescue radial formation (7/100 metaphases), nor did 53BP1$^{1052–1710}$ (10/100 metaphases), the oligomerization mutant 53BP1$^{\Delta 1231–1270}$ (12/100 metaphases), nor the alanine mutant 53BP1^{28A} (14/100 metaphases; Figure 7A). We conclude that the tudor, oligomerization domain and the S/T-Q sites at the N-terminus of 53BP1 are required for end protection and contribute to 53BP1-mediated toxicity in Brca1 mutant cells.

Discussion

DNA breaks jeopardize genomic integrity, yet they occur as by-products of DNA replication, oxidative metabolism, ionizing radiation and antigen receptor diversification reactions in lymphocytes (Hoeijmakers, 2009; Lieber, 2010; Nussenzweig and Nussenzweig, 2010). Joining of paired DNA breaks on disparate chromosomes leads to translocations, while joining paired intra-chromosomal breaks produces deletions that result in loss of genetic information. Translocations and deletions are commonly observed in cancer, where they are often recurrent and contribute to malignant transformation (Futreal et al., 2004).

HO, I-SceI, and zinc finger nucleases that produce unique DSBs in yeast and mammalian genomes have been used to explore the biology of chromosome translocations. However, much less is known about the role of DNA repair factors in protecting cells against intrachromosomal deletions. In the absence of a sister chromatid, DSBs are repaired by either C-NHEJ or A-NHEJ. The C-NHEJ pathway, requires DNA Ligase IV, XRCC4, Ku70 and Ku80, and is necessary for efficient repair of intrachromosomal DSBs as evidenced by reduced CSR when C-NHEJ is impaired (Boboila et al., 2010a; Boboila et al., 2010b). Contrary to its role in promoting intrachromosomal DSB repair, the C-NHEJ pathway inhibits chromosome translocations, which often harbor microhomologies at the translocation breakpoint indicative of joining by the A-NHEJ pathway (reviewed in (Kass and Jasin, 2010; Zhang et al., 2010) and (Ramiro et al., 2006)) To study the role of distance and DNA damage response factors in repair of tandem intra-chromosomal DSBs in mammalian cells we compared joining between I-SceI induced DSBs on chromosome 12 spaced by 1.2 kb, 96 kb, and 27 Mb. Our analysis reveals that DSBs 1.2 kb or 96 kb apart are more likely to join than those separated by 27 Mb. Indeed, when DSBs are separated by 27 Mb on chromosome 12 the rate of paired end joining in cis is similar to transchromosomal joining between *IgH* and *c-myc* on chromosome 15.

53BP1 facilitates end joining in cis (Bothmer et al., 2010); however, this effect is limited to DSBs separated by 96 kb, as loss of 53BP1 does not reduce the joining frequency of proximal, very distal or transchromosomal DSBs. The selective effect of 53BP1 on joining paired breaks separated by 96 kb suggests a role for DNA damage factors that spread along the chromosome in response to DSBs in an H2AX/RNF8 dependent manner (Bekker-Jensen et al., 2006; Savic et al., 2009). Indeed, the extent of γ-H2AX spreading from an I-SceI induced DSB at the IgH locus is confined to ~ 1 Mb surrounding the break (Figure S1I).

The new results are consistent with the finding that 53BP1 allows for a higher probability of interactions between DNA elements 28–172 kb apart during rearrangements of the TCRα locus (Difilippantonio et al., 2008). Since DSBs produced during CSR are separated by 60–200 kb, our findings support a model in which 53BP1 and possibly other focus forming

factors promote the synapsis of DSBs if they fall within the range of spread of the H2AX/RNF8 dependent DNA damage response. Interestingly, loss of 53BP1 does not affect recombination efficiency mediated by Cre/loxP, which is independent of the DNA damage response (Bothmer et al., 2010; Guo et al., 1997). This indicates that indeed 53BP1 acts downstream of a DSB, mediating synapsis of broken ends as part of the DNA damage response.

In addition to forming repair foci at DNA ends 53BP1 also protects DNA ends from resection and thereby favors repair by C-NHEJ while preventing A-NHEJ (a pathway with extensive processing and microhomology) and HR (Bothmer et al., 2010; Bunting et al., 2010). This may be particularly important during CSR in lymphocytes because switch regions are highly repetitive. Since 53BP1 protects ends from resection, its absence would favor micro-homology mediated intra-switch joining as opposed to productive switch recombination between different switch regions (Bothmer et al., 2010). However, end protection is not sufficient to explain the effects of 53BP1 on CSR since H2AX deficiency promotes extensive end resection (Figure 4B) and yet produces a milder CSR defect (Reina-San-Martin et al., 2003). Of note, all joining experiments were performed in the absence of AID, and we cannot exclude the possibility that AID, in addition to 53BP1, influences the repair pathway choice.

The way in which 53BP1 mediates end protection and facilitates joining was investigated by analyzing the contribution of the structural domains of 53BP1 to DNA end protection and class switching in B lymphocytes. Human 53BP1 binds to the histone mark $H4K20^{me2}$ via its tudor domain and mutation of amino acid D1521 in the tudor domain abrogates 53BP1's ability to form DNA damage foci in response to IR (Botuyan et al., 2006; Huyen et al., 2004). We find that 53BP1 is chromatin associated even in the absence of DNA damage or H2AX, which is consistent with previous reports showing that $H4K20^{me2}$ is a constitutive chromatin modification (Botuyan et al., 2006; Sanders et al., 2004) and that 53BP1 chromatin association is RNF8 and 53BP1-foci independent (Santos et al., 2010). These studies suggest that even in the context of undamaged chromatin this modification is accessible to 53BP1. Furthermore, a knock-in mutant of the tudor domain ($53BP1^{DR}$) that fails to form foci in response to DNA damage also fails to associate with chromatin in non-irradiated cells. Therefore, an intact tudor domain is required for both constitutive binding to chromatin and DNA damage induced focus formation. As predicted from its inability to bind chromatin or form DNA damage foci, $53BP1^{DR}$ was unable to protect DNA ends from resection or to support CSR.

The absence of 53BP1's oligomerization domain and deficiency in H2AX both impair the formation of stable DNA damage foci (Celeste et al., 2003; Fernandez-Capetillo et al., 2002; Ward et al., 2003; Yuan and Chen, 2010). In contrast, we find that neither the oligomerization domain of 53BP1 nor H2AX are required for 53BP1 binding to chromatin. However, DNA end protection and CSR are impaired in the absence of either. Thus the ability to bind constitutively to chromatin appears to be necessary but not sufficient for end protection or CSR. Consistent with this idea, a fragment of 53BP1, which binds chromatin and forms DNA damage inducible foci ($53BP1^{1052–1710}$), is unable to support either end protection or CSR. Interestingly and unlike 53BP1, H2AX deficiency does not rescue the formation of radial fusions observed in PARP inhibitor treated Brca1 mutant B cells (Figure 4C). Although H2AX and 53BP1 deficiency both lead to increased end-resection (Bothmer et al., 2010; Bunting et al., 2010; Helmink et al., 2011; Zha et al., 2011), H2AX in contrast to 53BP1 likely plays additional roles in HR and NHEJ which may be essential in Brca1 deficient cells. Similar to H2AX, RNF8 and RNF168 are required for stable 53BP1 focus formation upon IR (Doil et al., 2009; Huen et al., 2007; Kolas et al., 2007; Mailand et al., 2007; Stewart et al., 2009; Yuan and Chen, 2010). In this context, it will be interesting to

test the effect of RNF8/RNF168 deficiency on PARP inhibitor induced chromosome abnormalities in Brca1$^{\Delta 11/\Delta 11}$ cells, as these ubiquitin ligases lie downstream of H2AX and upstream of 53BP1.

Our analysis of tandem BRCT domains mutant B cells (53BP1$^{\Delta BRCT}$) showed that the C-terminus is dispensable for both CSR and the protection of ends from processing, which suggests a role for the N-terminus in these processes. The N-terminus of 53BP1 lacks known structural domains, but contains S/T-Q consensus target sites for ATM phosphorylation that are implicated in promoting the resolution of γ-H2AX foci upon IR (DiTullio et al., 2002; Morales et al., 2003; Ward et al., 2006). We find that the putative ATM phosphorylation sites are also required to prevent DNA resection and to support CSR, suggesting that N-terminally phosphorylated 53BP1 may recruit additional factors to regulate DNA repair. In summary (Figure 7B), out of all the 53BP1 functional domains tested, the ability to protect DNA ends from resection is the only parameter that correlates with CSR. Chromatin association, focus formation, oligomerization, and intact N-terminal ATM phosporylation sites are all essential but by themselves not sufficient to prevent DNA end processing or to support CSR. Therefore, end protection and CSR may not simply be mediated by direct physical association of 53BP1 with DNA ends but appears to require the assembly of a complex composed of H2AX, 53BP1 and possibly additional yet-to-be defined proteins.

Experimental Procedures

Mice

IgH$^{I\text{-}1k/+}$, IgH$^{I\text{-}27M/+}$, 53BP1$^{\Delta BRCT/+}$, 53BP1$^{DR/+}$, and 53BP1$^{\Delta 1210–1447/+}$ mice were generated by homologous recombination in C57BL/6 albino embryonic stem (ES) cells. Details of the targeting vectors, screening by Southern blot, and genotyping PCR are provided in the legends to the Supplemental Data. IgH$^{I\text{-}96k/+}$ (Bothmer et al., 2010), IgH$^{I/+}$ and Myc$^{I/+}$ (Robbiani et al., 2008), AID$^{-/-}$ (Muramatsu et al., 2000), 53BP1$^{-/-}$ (Ward et al., 2004), H2AX$^{-/-}$ (Celeste et al., 2002), Brca1$^{lox/lox}$ (Xu et al., 1999), Brca1$^{\Delta 11/\Delta 11}$ (Xu et al., 2001), and CD19^{cre} mice (Rickert et al., 1997) were previously described. Unless otherwise indicated, experiments were performed with mice homozygous for the indicated alleles. All experiments were performed in accordance with protocols approved by the Rockefeller University and National Institutes of Health (NIH) Institutional Animal Care and Use Committee.

Joining and Resection Analysis

The assay was performed as previously described (Bothmer et al., 2010). For details see supplement.

B Cell Cultures and Retroviral Transduction

Resting B lymphocytes were isolated and stimulated for CSR as previously described (Robbiani et al., 2008). For analysis of radial structures the PARP inhibitor KU58948 (1 μM) was added 16 hr before, and Colcemid (100 ng/ml, Roche) 1 hour before preparation of metaphase spreads (Bunting et al., 2010). For infection experiments, retroviral supernatants were prepared and administered as previously described (Robbiani et al., 2008). B cells were analyzed at 96 hr from the beginning of their culture.

Retroviruses

pMX-IRES-GFP based retroviruses encoding for I-SceI and catalytic mutant I-SceI* were previously described (Robbiani et al., 2008). Coding sequences of the human 53BP1 mutants were cloned into a modified pMX plasmid with deleted IRES-GFP (courtesy of Dr. Silvia Boscardin), to allow for proper packaging of this large protein. Therefore, in each

experiment infection efficiency was monitored by Western Blot (see supplemental figures). 53BP1^{8A} encoded for the following alanine substitutions: S6A; S13A; S25A; S29A; S105A; S166A; S176A; S178A. 53BP1^{7A} encoded for: T302A; S452A; S523A; S543A; S625A; S784A; S892A. 53BP1^{15A} encoded for the same alanine substitutions as in both 53BP1^{8A} and 53BP1^{7A}. In addition to these, 53BP1^{28A} also had S437A; S580A; S674A; T696A; S698A; S831A; T855A; S1068A; S1086A; S1104A; S1148A; T1171A; S1219A. Unless otherwise noted, mutants bore a C-terminal HA-FLAG tag (in orange in Figures 5C, 6A and S6A).

Cell Fractionation and Western Blot

The cytoplasmic fraction from 5 Mio purified mutant splenic B cells (treated or not with 10 Gy IR and allowed 90 min recovery) was separated from the nuclei using the ProteoJET Cytoplasmic and Nuclear Protein Extraction Kit (Fermentas) following the manufacturer's instructions. To separate nuclear-soluble and chromatin fractions, the manufacturer's nuclei lysis buffer was supplemented with the provided Nuclei Lysis reagent and with 30 mM EDTA, 2 mM EGTA, and 10 mM dithiothreitol. The nuclear extract was centrifuged at 1700 g for 20 min at 4° C; the supernatant was saved at −80º C as the "nuclear-soluble fraction", and the chromatin pellet was washed twice in 250 μl of 3 mM EDTA, 0.2 mM EGTA, 1 mM dithiothreitol, and protease inhibitors (Roche). Chromatin was resuspended in 30 μl of 10 mM Hepes, 10 mM KCl, 1 mM $MgCl_2$, 10% glycerol, 1 mM $CaCl_2$, 1 mM EDTA, 1× protease inhibitors (Roche), and 5 U of micrococcal nuclease (New England Biolabs), and then incubated for 45 min at 37° C. The reaction was stopped by the addition of EGTA to 1 mM, and the digested pellet was stored at −80° C as the "chromatin-bound fraction." For retroviral reconstitution experiments, splenocytes were stimulated and fractionated on day 4. Expression of wild type and mutant 53BP1 proteins was detected with antisera to 53BP1 (Bethyl), 53BP1 phosphorylated on Serine 25 (Bethyl), FLAG (SIGMA), or HA (Abcam), as indicated. Controls for DNA damage, cell fractionation and for loading were with antibodies to γ-H2AX (Millipore), H2AX (Bethyl), H4K20^{me1} (Abcam), IgG LC (Jackson Immunoresearch Laboratories), tubulin (Abcam) or actin (SIGMA).

Flow Cytometry

For fluorescence-activated cell sorting (FACS) analysis, spleen cell suspensions or cultures were stained with fluorochrome-conjugated anti-CD19, anti-CD3, anti-IgM, anti-IgD, and anti-IgG1 (Pharmingen). Labeling for cell division was at 37° C for 10 min in 5 μM carboxyfluorescein succinimidyl esther (CFSE). Samples were acquired on a FACSCalibur instrument (Becton Dickinson) and analyzed with FlowJo software (Tree Star).

Ionizing Radiation Induced Foci and Laser Microirradiation

For IRIF, mouse embryonic fibroblasts (MEFs) were grown overnight on glass coverslips in 30mm culture dishes, then exposed to 5 Gy (53BP1 mutant MEFs) or 10 Gy (53BP1$^{-/-}$ MEFs reconstituted with mutant retroviruses) ionizing radiation and allowed to recover for 90 min. Cells were then fixed with 4% paraformaldehyde, followed by 0.5% Triton X-100 permeabilzation and processed for immunofluorescent staining at the indicated times after exposure. Images were acquired using an LSM 510 META microscope (Zeiss) or with DeltaVision (Applied Precision). For laser microirradiation, MEFs were grown in dye-free media. The DNA binding dye Hoechst 33258 was added at 10 mg/ml and incubated for 30 min at 37° C. After laser treatment, cells were allowed to recover for 30 min or 4 h at 37° C and were subsequently fixed and processed for immunofluorescent staining as above. Primary antibodies used for immunofluorescence were rabbit anti-53BP1 (Novus Biologicals), mouse anti-γ-H2AX (Upstate Biotechnology), and mouse anti-FLAG-M2 (SIGMA). Secondary antibodies were Alexa568- and Alexa488-conjugated (Molecular Probes). DNA was counterstained with 4′,6-diamidino-2-phenylindole (DAPI).

Supplementary Material

Refer to Web version on PubMed Central for supplementary material.

Acknowledgments

All members of the Nussenzweig labs for discussions. Dr. Thanos Halazonetis for wild type human 53BP1 plasmid and Dr. Philip Carpenter for plasmid with 53BP1 alanine substitutions. The Rockefeller University Gene Targeting Facility for the generation of mutant mice. The work was supported in part by a Fondazione Ettore e Valeria Rossi grant to D.F.R., by NIH grant to M.C.N (AI037526) and DOD grant to A.N (BC102335). A.N. and S.B. were supported by the Intramural research Program of the NIH, National Cancer Institute and the Center for Cancer Research and I.A.K by NIH MSTP grant GM07739. A.B. is a predoctoral Fellow of the Cancer Research Institute, N.F. is and D.F.R. was a Fellow of the Leukemia and Lymphoma Society, M.D.V. is a Fellow of the American-Italian Cancer Foundation, and M.C.N. is an HHMI Investigator.

References

Adams MM, Carpenter PB. Tying the loose ends together in DNA double strand break repair with 53BP1. Cell Div. 2006; 1:19. [PubMed: 16945145]

Anderson L, Henderson C, Adachi Y. Phosphorylation and rapid relocalization of 53BP1 to nuclear foci upon DNA damage. Mol Cell Biol. 2001; 21:1719–1729. [PubMed: 11238909]

Bekker-Jensen S, Lukas C, Kitagawa R, Melander F, Kastan MB, Bartek J, Lukas J. Spatial organization of the mammalian genome surveillance machinery in response to DNA strand breaks. J Cell Biol. 2006; 173:195–206. [PubMed: 16618811]

Boboila C, Jankovic M, Yan CT, Wang JH, Wesemann DR, Zhang T, Fazeli A, Feldman L, Nussenzweig A, Nussenzweig M, Alt FW. Alternative end-joining catalyzes robust IgH locus deletions and translocations in the combined absence of ligase 4 and Ku70. Proc Natl Acad Sci U S A. 2010a; 107:3034–3039. [PubMed: 20133803]

Boboila C, Yan C, Wesemann DR, Jankovic M, Wang JH, Manis J, Nussenzweig A, Nussenzweig M, Alt FW. Alternative end-joining catalyzes class switch recombination in the absence of both Ku70 and DNA ligase 4. J Exp Med. 2010b; 207:417–427. [PubMed: 20142431]

Boisvert FM, Rhie A, Richard S, Doherty AJ. The GAR motif of 53BP1 is arginine methylated by PRMT1 and is necessary for 53BP1 DNA binding activity. Cell Cycle. 2005; 4:1834–1841. [PubMed: 16294045]

Bothmer A, Robbiani DF, Feldhahn N, Gazumyan A, Nussenzweig A, Nussenzweig MC. 53BP1 regulates DNA resection and the choice between classical and alternative end joining during class switch recombination. J Exp Med. 2010; 207:855–865. [PubMed: 20368578]

Botuyan MV, Lee J, Ward IM, Kim JE, Thompson JR, Chen J, Mer G. Structural basis for the methylation state-specific recognition of histone H4-K20 by 53BP1 and Crb2 in DNA repair. Cell. 2006; 127:1361–1373. [PubMed: 17190600]

Bunting SF, Callen E, Wong N, Chen HT, Polato F, Gunn A, Bothmer A, Feldhahn N, Fernandez-Capetillo O, Cao L, et al. 53BP1 inhibits homologous recombination in Brca1-deficient cells by blocking resection of DNA breaks. Cell. 2010; 141:243–254. [PubMed: 20362325]

Celeste A, Fernandez-Capetillo O, Kruhlak MJ, Pilch DR, Staudt DW, Lee A, Bonner RF, Bonner WM, Nussenzweig A. Histone H2AX phosphorylation is dispensable for the initial recognition of DNA breaks. Nat Cell Biol. 2003; 5:675–679. [PubMed: 12792649]

Celeste A, Petersen S, Romanienko PJ, Fernandez-Capetillo O, Chen HT, Sedelnikova OA, Reina-San-Martin B, Coppola V, Meffre E, Difilippantonio MJ, et al. Genomic instability in mice lacking histone H2AX. Science. 2002; 296:922–927. [PubMed: 11934988]

Difilippantonio S, Gapud E, Wong N, Huang CY, Mahowald G, Chen HT, Kruhlak MJ, Callen E, Livak F, Nussenzweig MC, et al. 53BP1 facilitates long-range DNA end-joining during V(D)J recombination. Nature. 2008; 456:529–533. [PubMed: 18931658]

Dimitrova N, Chen YC, Spector DL, de Lange T. 53BP1 promotes non-homologous end joining of telomeres by increasing chromatin mobility. Nature. 2008; 456:524–528. [PubMed: 18931659]

DiTullio RA Jr, Mochan TA, Venere M, Bartkova J, Sehested M, Bartek J, Halazonetis TD. 53BP1 functions in an ATM-dependent checkpoint pathway that is constitutively activated in human cancer. Nat Cell Biol. 2002; 4:998–1002. [PubMed: 12447382]

Doil C, Mailand N, Bekker-Jensen S, Menard P, Larsen DH, Pepperkok R, Ellenberg J, Panier S, Durocher D, Bartek J, et al. RNF168 binds and amplifies ubiquitin conjugates on damaged chromosomes to allow accumulation of repair proteins. Cell. 2009; 136:435–446. [PubMed: 19203579]

Fernandez-Capetillo O, Chen HT, Celeste A, Ward I, Romanienko PJ, Morales JC, Naka K, Xia Z, Camerini-Otero RD, Motoyama N, et al. DNA damage-induced G2-M checkpoint activation by histone H2AX and 53BP1. Nat Cell Biol. 2002; 4:993–997. [PubMed: 12447390]

Futreal PA, Coin L, Marshall M, Down T, Hubbard T, Wooster R, Rahman N, Stratton MR. A census of human cancer genes. Nat Rev Cancer. 2004; 4:177–183. [PubMed: 14993899]

Guo F, Gopaul DN, van Duyne GD. Structure of Cre recombinase complexed with DNA in a site-specific recombination synapse. Nature. 1997; 389:40–46. [PubMed: 9288963]

Helmink BA, Tubbs AT, Dorsett Y, Bednarski JJ, Walker LM, Feng Z, Sharma GG, McKinnon PJ, Zhang J, Bassing CH, Sleckman BP. H2AX prevents CtIP-mediated DNA end resection and aberrant repair in G1-phase lymphocytes. Nature. 2011; 469:245–249. [PubMed: 21160476]

Hoeijmakers JH. DNA damage, aging, and cancer. N Engl J Med. 2009; 361:1475–1485. [PubMed: 19812404]

Huen MS, Grant R, Manke I, Minn K, Yu X, Yaffe MB, Chen J. RNF8 transduces the DNA-damage signal via histone ubiquitylation and checkpoint protein assembly. Cell. 2007; 131:901–914. [PubMed: 18001825]

Huen MS, Huang J, Leung JW, Sy SM, Leung KM, Ching YP, Tsao SW, Chen J. Regulation of chromatin architecture by the PWWP domain-containing DNA damage-responsive factor EXPAND1/MUM1. Mol Cell. 2010; 37:854–864. [PubMed: 20347427]

Huyen Y, Zgheib O, Ditullio RA Jr, Gorgoulis VG, Zacharatos P, Petty TJ, Sheston EA, Mellert HS, Stavridi ES, Halazonetis TD. Methylated lysine 79 of histone H3 targets 53BP1 to DNA double-strand breaks. Nature. 2004; 432:406–411. [PubMed: 15525939]

Iwabuchi K, Basu BP, Kysela B, Kurihara T, Shibata M, Guan D, Cao Y, Hamada T, Imamura K, Jeggo PA, et al. Potential role for 53BP1 in DNA end-joining repair through direct interaction with DNA. J Biol Chem. 2003; 278:36487–36495. [PubMed: 12824158]

Kass EM, Jasin M. Collaboration and competition between DNA double-strand break repair pathways. FEBS Lett. 2010; 584:3703–3708. [PubMed: 20691183]

Kolas NK, Chapman JR, Nakada S, Ylanko J, Chahwan R, Sweeney FD, Panier S, Mendez M, Wildenhain J, Thomson TM, et al. Orchestration of the DNA-damage response by the RNF8 ubiquitin ligase. Science. 2007; 318:1637–1640. [PubMed: 18006705]

Lee H, Kwak HJ, Cho IT, Park SH, Lee CH. S1219 residue of 53BP1 is phosphorylated by ATM kinase upon DNA damage and required for proper execution of DNA damage response. Biochem Biophys Res Commun. 2009; 378:32–36. [PubMed: 18996087]

Lieber MR. The mechanism of double-strand DNA break repair by the nonhomologous DNA end-joining pathway. Annu Rev Biochem. 2010; 79:181–211. [PubMed: 20192759]

Mailand N, Bekker-Jensen S, Faustrup H, Melander F, Bartek J, Lukas C, Lukas J. RNF8 ubiquitylates histones at DNA double-strand breaks and promotes assembly of repair proteins. Cell. 2007; 131:887–900. [PubMed: 18001824]

Manis JP, Morales JC, Xia Z, Kutok JL, Alt FW, Carpenter PB. 53BP1 links DNA damage-response pathways to immunoglobulin heavy chain class-switch recombination. Nat Immunol. 2004; 5:481–487. [PubMed: 15077110]

Morales JC, Xia Z, Lu T, Aldrich MB, Wang B, Rosales C, Kellems RE, Hittelman WN, Elledge SJ, Carpenter PB. Role for the BRCA1 C-terminal repeats (BRCT) protein 53BP1 in maintaining genomic stability. J Biol Chem. 2003; 278:14971–14977. [PubMed: 12578828]

Muramatsu M, Kinoshita K, Fagarasan S, Yamada S, Shinkai Y, Honjo T. Class switch recombination and hypermutation require activation-induced cytidine deaminase (AID), a potential RNA editing enzyme. Cell. 2000; 102:553–563. [PubMed: 11007474]

Nussenzweig A, Nussenzweig MC. Origin of chromosomal translocations in lymphoid cancer. Cell. 2010; 141:27–38. [PubMed: 20371343]

Ramiro AR, Jankovic M, Callen E, Difilippantonio S, Chen HT, McBride KM, Eisenreich TR, Chen J, Dickins RA, Lowe SW, et al. Role of genomic instability and p53 in AID-induced c-myc-Igh translocations. Nature. 2006; 440:105–109. [PubMed: 16400328]

Rappold I, Iwabuchi K, Date T, Chen J. Tumor suppressor p53 binding protein 1 (53BP1) is involved in DNA damage-signaling pathways. J Cell Biol. 2001; 153:613–620. [PubMed: 11331310]

Reina-San-Martin B, Chen J, Nussenzweig A, Nussenzweig MC. Enhanced intra-switch region recombination during immunoglobulin class switch recombination in 53BP1−/− B cells. Eur J Immunol. 2007; 37:235–239. [PubMed: 17183606]

Reina-San-Martin B, Difilippantonio S, Hanitsch L, Masilamani RF, Nussenzweig A, Nussenzweig MC. H2AX is required for recombination between immunoglobulin switch regions but not for intra-switch region recombination or somatic hypermutation. J Exp Med. 2003; 197:1767–1778. [PubMed: 12810694]

Rickert RC, Roes J, Rajewsky K. B lymphocyte-specific, Cre-mediated mutagenesis in mice. Nucleic Acids Res. 1997; 25:1317–1318. [PubMed: 9092650]

Robbiani DF, Bothmer A, Callen E, Reina-San-Martin B, Dorsett Y, Difilippantonio S, Bolland DJ, Chen HT, Corcoran AE, Nussenzweig A, Nussenzweig MC. AID is required for the chromosomal breaks in c-myc that lead to c-myc/IgH translocations. Cell. 2008; 135:1028–1038. [PubMed: 19070574]

Sanders SL, Portoso M, Mata J, Bahler J, Allshire RC, Kouzarides T. Methylation of histone H4 lysine 20 controls recruitment of Crb2 to sites of DNA damage. Cell. 2004; 119:603–614. [PubMed: 15550243]

Santos MA, Huen MS, Jankovic M, Chen HT, Lopez-Contreras AJ, Klein IA, Wong N, Barbancho JL, Fernandez-Capetillo O, Nussenzweig MC, et al. Class switching and meiotic defects in mice lacking the E3 ubiquitin ligase RNF8. J Exp Med. 2010; 207:973–981. [PubMed: 20385748]

Savic V, Yin B, Maas NL, Bredemeyer AL, Carpenter AC, Helmink BA, Yang-Iott KS, Sleckman BP, Bassing CH. Formation of dynamic gamma-H2AX domains along broken DNA strands is distinctly regulated by ATM and MDC1 and dependent upon H2AX densities in chromatin. Mol Cell. 2009; 34:298–310. [PubMed: 19450528]

Schultz LB, Chehab NH, Malikzay A, Halazonetis TD. p53 binding protein 1 (53BP1) is an early participant in the cellular response to DNA double-strand breaks. J Cell Biol. 2000; 151:1381–1390. [PubMed: 11134068]

Stavnezer J, Guikema JE, Schrader CE. Mechanism and Regulation of Class Switch Recombination. Annu Rev Immunol. 2008; 26:261–292. [PubMed: 18370922]

Stewart GS, Panier S, Townsend K, Al-Hakim AK, Kolas NK, Miller ES, Nakada S, Ylanko J, Olivarius S, Mendez M, et al. The RIDDLE syndrome protein mediates a ubiquitin-dependent signaling cascade at sites of DNA damage. Cell. 2009; 136:420–434. [PubMed: 19203578]

Ward I, Kim JE, Minn K, Chini CC, Mer G, Chen J. The tandem BRCT domain of 53BP1 is not required for its repair function. J Biol Chem. 2006; 281:38472–38477. [PubMed: 17043355]

Ward IM, Minn K, Jorda KG, Chen J. Accumulation of checkpoint protein 53BP1 at DNA breaks involves its binding to phosphorylated histone H2AX. J Biol Chem. 2003; 278:19579–19582. [PubMed: 12697768]

Ward IM, Reina-San-Martin B, Olaru A, Minn K, Tamada K, Lau JS, Cascalho M, Chen L, Nussenzweig A, Livak F, et al. 53BP1 is required for class switch recombination. J Cell Biol. 2004; 165:459–464. [PubMed: 15159415]

Watanabe K, Iwabuchi K, Sun J, Tsuji Y, Tani T, Tokunaga K, Date T, Hashimoto M, Yamaizumi M, Tateishi S. RAD18 promotes DNA double-strand break repair during G1 phase through chromatin retention of 53BP1. Nucleic Acids Res. 2009; 37:2176–2193. [PubMed: 19228710]

Xu X, Qiao W, Linke SP, Cao L, Li WM, Furth PA, Harris CC, Deng CX. Genetic interactions between tumor suppressors Brca1 and p53 in apoptosis, cell cycle and tumorigenesis. Nat Genet. 2001; 28:266–271. [PubMed: 11431698]

Xu X, Wagner KU, Larson D, Weaver Z, Li C, Ried T, Hennighausen L, Wynshaw-Boris A, Deng CX. Conditional mutation of Brca1 in mammary epithelial cells results in blunted ductal morphogenesis and tumour formation. Nat Genet. 1999; 22:37–43. [PubMed: 10319859]

Yuan J, Chen J. MRE11-RAD50-NBS1 complex dictates DNA repair independent of H2AX. J Biol Chem. 2010; 285:1097–1104. [PubMed: 19910469]

Zgheib O, Pataky K, Brugger J, Halazonetis TD. An oligomerized 53BP1 tudor domain suffices for recognition of DNA double-strand breaks. Mol Cell Biol. 2009; 29:1050–1058. [PubMed: 19064641]

Zha S, Guo C, Boboila C, Oksenych V, Cheng HL, Zhang Y, Wesemann DR, Yuen G, Patel H, Goff PH, et al. ATM damage response and XLF repair factor are functionally redundant in joining DNA breaks. Nature. 2011; 469:250–254. [PubMed: 21160472]

Zhang Y, Gostissa M, Hildebrand DG, Becker MS, Boboila C, Chiarle R, Lewis S, Alt FW. The role of mechanistic factors in promoting chromosomal translocations found in lymphoid and other cancers. Adv Immunol. 2010; 106:93–133. [PubMed: 20728025]

Highlights

- 53BP1 facilitates the joining of DSBs depending on the distance between breaks
- 53BP1 prevents DNA end resection independent of the distance between breaks
- In the absence of H2AX, 53BP1 is chromatin associated but does not block resection
- multiple functions of 53BP1 are needed for end protection and Ig class switching

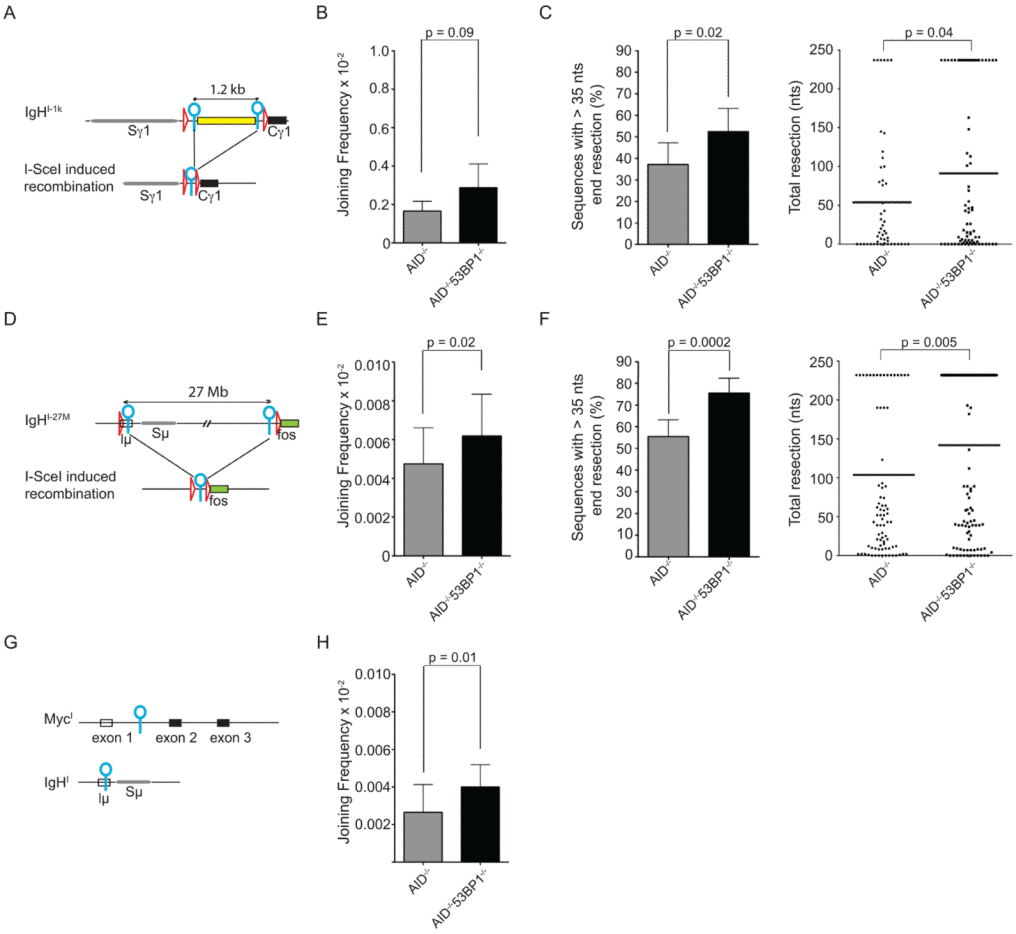

Figure 1. 53BP1 effects on joining efficiency of proximal (1 kb) or distal (27 Mb) DSBs

(A) Schematic representation of $IgH^{I\text{-}1k}$ allele before (top) and after (bottom) I-SceI induced recombination. I-SceI sites are indicated as blue circles, loxP sites as red triangles. Spacer sequence of 1.2 kb is indicated as yellow rectangle. **(B)** Bar graph shows I-SceI induced recombination frequency of $IgH^{I\text{-}1k/+}AID^{-/-}$ B cells in the presence or absence of 53BP1. P value was calculated using a paired two tailed students t-test. See also panel S1F. **(C)** Left: Bar graph showing the frequency of I-SceI induced recombination products with more than 35 nts end processing for $IgH^{I\text{-}1k/+}AID^{-/-}$ and $IgH^{I\text{-}1k/+}AID^{-/-}53BP1^{-/-}$ B cells. Right: Dot plot showing resection in sequences from I-SceI infected $IgH^{I\text{-}1k/+}AID^{-/-}$ and $IgH^{I\text{-}1k/+}AID^{-/-}53BP1^{-/-}$ B cells, with each dot representing one cloned sequence. **(D)** Schematic representation of $IgH^{I\text{-}27M}$ allele before (top) and after (bottom) I-SceI induced recombination. **(E)** As in **(B)** for $IgH^{I\text{-}27M/+}AID^{-/-}$ and $IgH^{I\text{-}27M/+}AID^{-/-}53BP1^{-/-}$ B cells. See also panel S1G. **(F)** As in **(C)** for $IgH^{I\text{-}27M/+}AID^{-/-}$ and $IgH^{I\text{-}27M/+}AID^{-/-}53BP1^{-/-}$ B cells. **(G)** Schematic representation of the Myc^{I} and IgH^{I} alleles. **(H)** As in **(B and E)** for $IgH^{I/+}Myc^{I/+}AID^{-/-}$ B cells in the presence and absence of 53BP1. See also panel S1H. In all figures: Horizontal lines in dot plots indicate the means; **Error bars indicate standard deviations**; p values were calculated using a two-tailed students t-test, unless otherwise indicated; All graphs represent data from at least three independent experiments, unless specified. See also Figure S1.

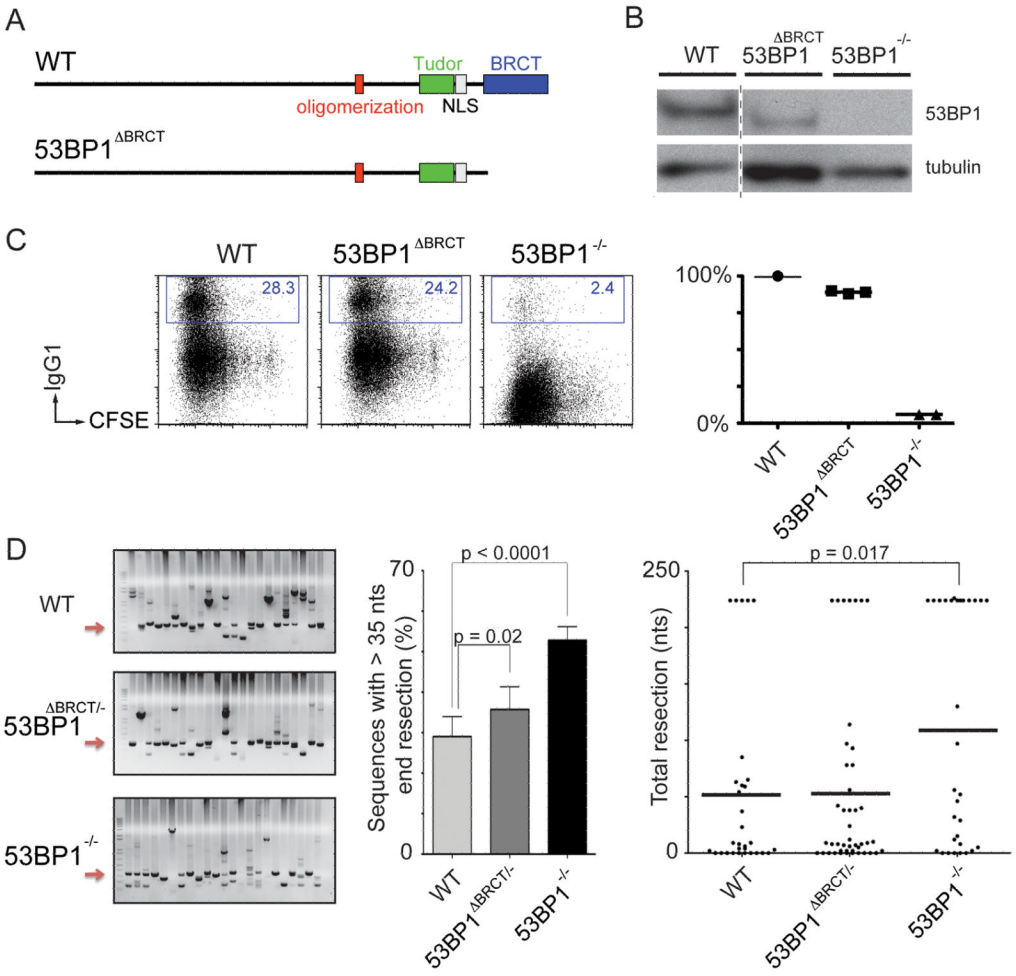

Figure 2. The BRCT domains are dispensable for CSR and DNA end protection

(A) Schematic representation of wild type (WT) 53BP1 protein (top) and 53BP1 lacking the BRCT domains (bottom). **(B)** Western blot showing 53BP1 expression levels in WT and 53BP1$^{\Delta BRCT}$ B cells. **(C)** Left: Representative flow cytometry plots measuring CSR after stimulation of WT, 53BP1$^{\Delta BRCT}$ and 53BP1$^{-/-}$ B cells. Numbers indicate the percentage of IgG1 switched cells. CFSE dye tracks cell division. Right: Summary dot plot indicating CSR as a percentage of WT value within the same experiment. Each dot represents an independent experiment. **(D)** Left: Representative ethidium bromide stained argarose gels showing PCR products obtained after I-SceI induced recombination in IgH$^{I\text{-}96k/+}$, IgH$^{I\text{-}96k/+}$53BP1$^{\Delta BRCT/-}$ and IgH$^{I\text{-}96k}$53BP1$^{-/-}$ B cells. Middle: Bar graph quantitating the frequency of I-SceI induced recombination products with more than 35 nts end processing. **Error bars indicate standard deviation.** Right: Dot plot showing resection with each dot representing one sequence. Two independent experiments. See also Figure S2.

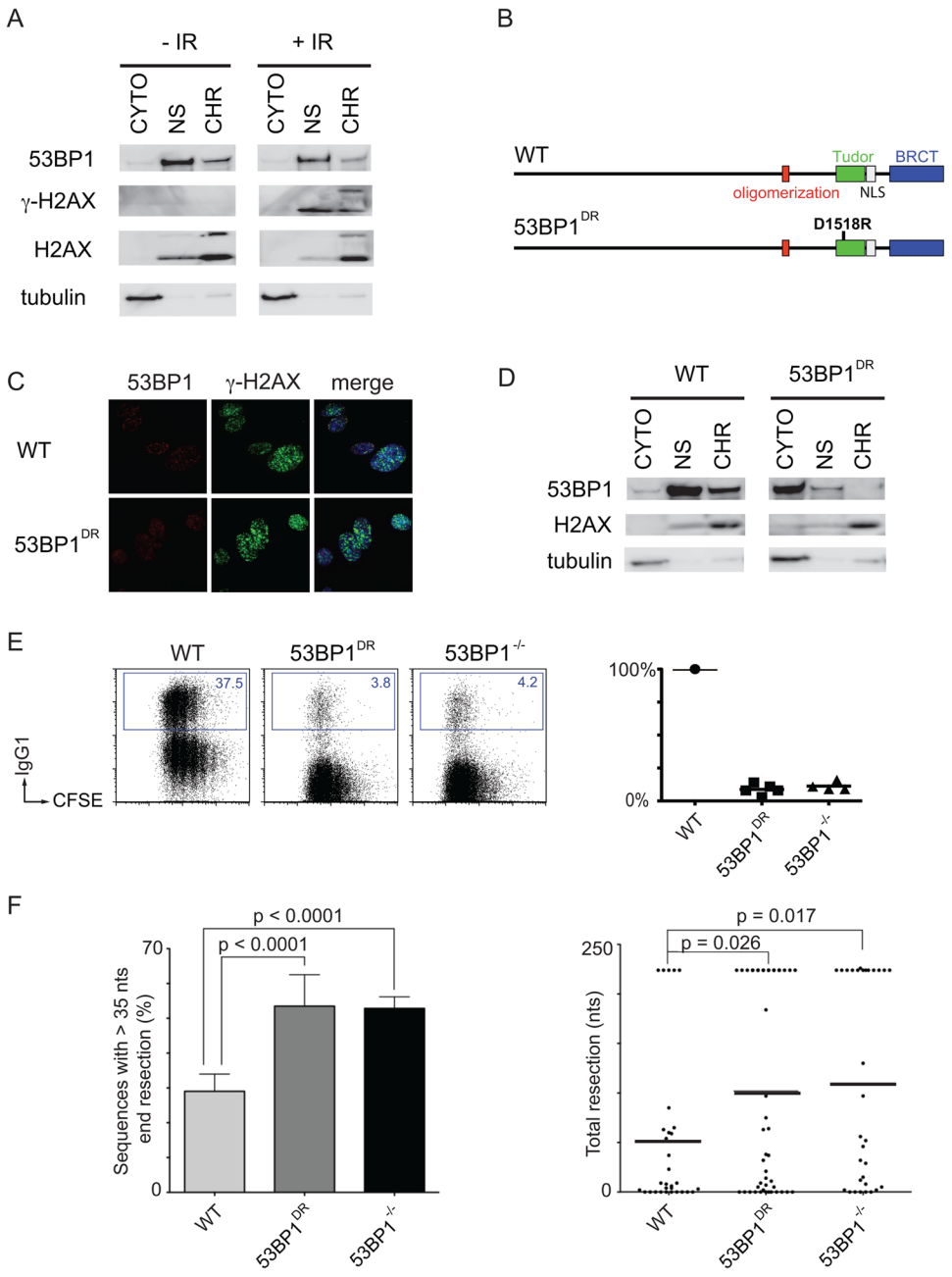

Figure 3. 53BP1 tudor domains are required for CSR and for the protection of DNA ends

(A) Western blots of fractionated WT B cells +/− 10 Gy of IR. CYTO, cytoplasmic fraction; NS, nuclear soluble fraction; CHR, chromatin fraction. **(B)** Schematic representation of WT 53BP1 (top) and 53BP1 with tudor domain mutation D1518R (bottom). **(C)** 53BP1 and γ-H2AX IRIF in WT and 53BP1^{DR} MEFs after IR. **(D)** Western blots of unstimulated, fractionated WT and 53BP1^{DR} B cells. **(E)** Left: Representative flow cytometry plots measuring CSR to IgG1 after stimulation of WT, 53BP1^{DR} and 53BP1$^{-/-}$ B cells. Right: Summary dot plot indicating CSR as a percentage of WT. Each dot represents an independent experiment. **(F)** As in Figure 1(C) for WT, 53BP1^{DR} and 53BP1$^{-/-}$ B cells. **Error bars indicate standard deviation.** Two independent experiments. See also Figure S3.

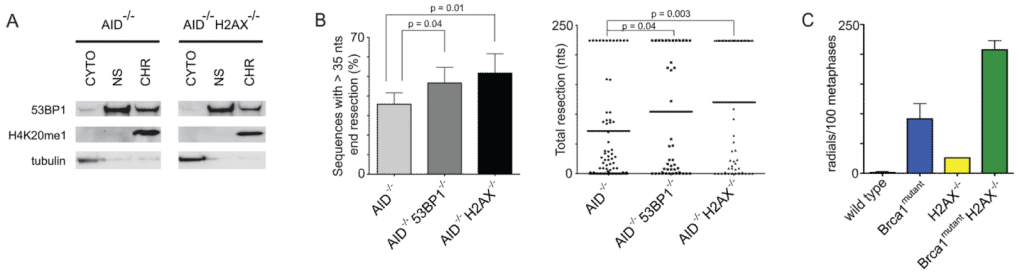

Figure 4. 53BP1 chromatin association in the absence of H2AX is not sufficient to prevent end resection

(A) Western blots of fractionated $AID^{-/-}$ and $AID^{-/-}H2AX^{-/-}$ B cells. **(B)** Left: Bar graph showing the frequency of I-SceI induced recombination products with more than 35 nts end processing for $IgH^{I\text{-}96k/+}AID^{-/-}$, $IgH^{I\text{-}96k/+}AID^{-/-}53BP1^{-/-}$ and $IgH^{I\text{-}96k/+}AID^{-/-}H2AX^{-/-}$ B cells. Right: Dot plot showing resection in sequences from I-SceI infected $IgH^{I\text{-}96k/+}AID^{-/-}$, $IgH^{I\text{-}96k/+}AID^{-/-}53BP1^{-/-}$ and $IgH^{I\text{-}96k/+}AID^{-/-}H2AX^{-/-}$ B cells. **Error bars indicate standard error of the mean.** Two independent experiments. **(C)** Histogram with number of radial structures in metaphases from PARP inhibitor treated $Brca1^{lox/lox}CD19^{cre/+}$ (= $Brca1^{mutant}$) B cells either proficient or deficient for H2AX. **Error bars indicate standard error of the mean.** Two independent experiments.

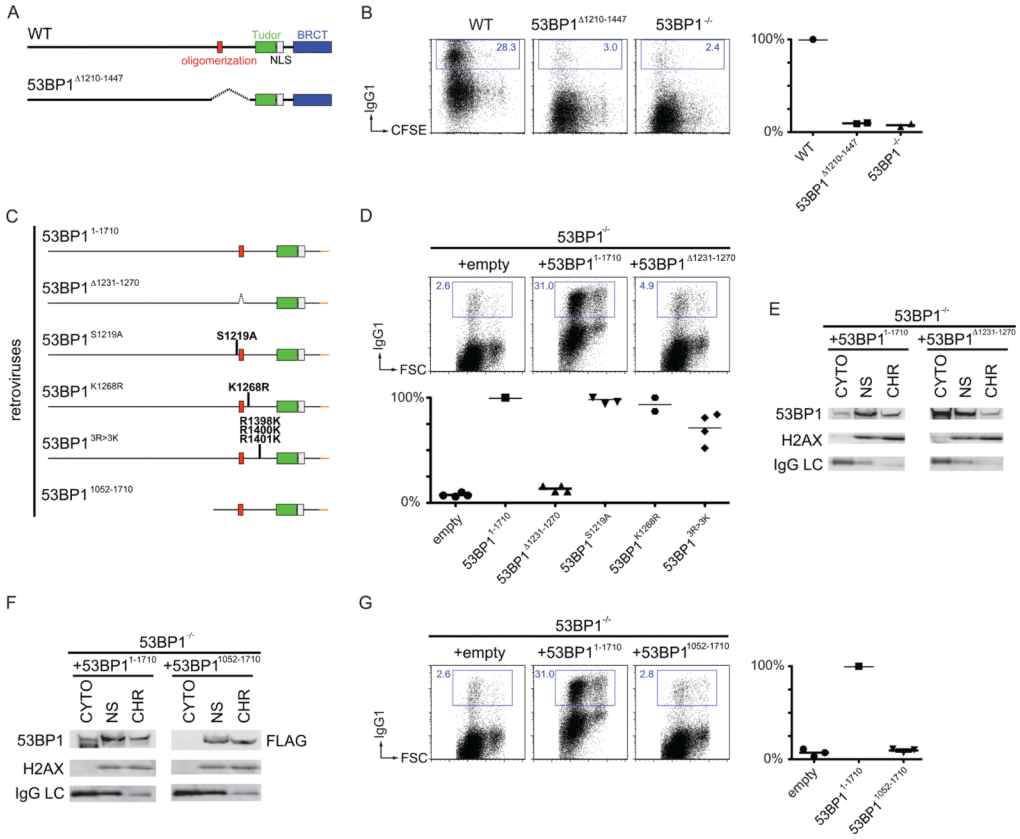

Figure 5. The oligomerization domain of 53BP1 in chromatin association and CSR

(A) Schematic representation of WT 53BP1 (top) and 53BP1 lacking amino acids 1210–1447 (bottom). **(B)** As in Figure 2(C) for WT, 53BP1$^{\Delta 1210–1447}$ and 53BP1$^{-/-}$ B cells. **(C)** Diagram of 53BP1 retroviral constructs with the indicated mutations and deletions. **(D)** As in Figure 2(C) after infection of 53BP1$^{-/-}$ B cells with empty retrovirus, or retrovirus expressing 53BP1$^{1–1710}$, or the oligomerization mutant 53BP1$^{\Delta 1231–1270}$, or the other mutants listed in panel **(C). (E)** Western blots of fractionated 53BP1$^{-/-}$ B cells stimulated and infected with 53BP1$^{1–1710}$ or 53BP1$^{\Delta 1231–1270}$. **(F)** Western blots of fractionated 53BP1$^{-/-}$ B cells stimulated and infected with 53BP1$^{1–1710}$ or 53BP1$^{1052–1710}$. **(G)** As in Figure 2(C) after infection of 53BP1$^{-/-}$ B cells with empty retrovirus, or retroviruses expressing 53BP1$^{1–1710}$ or the N-terminal deleted mutant 53BP1$^{1052–1710}$. See also Figure S4.

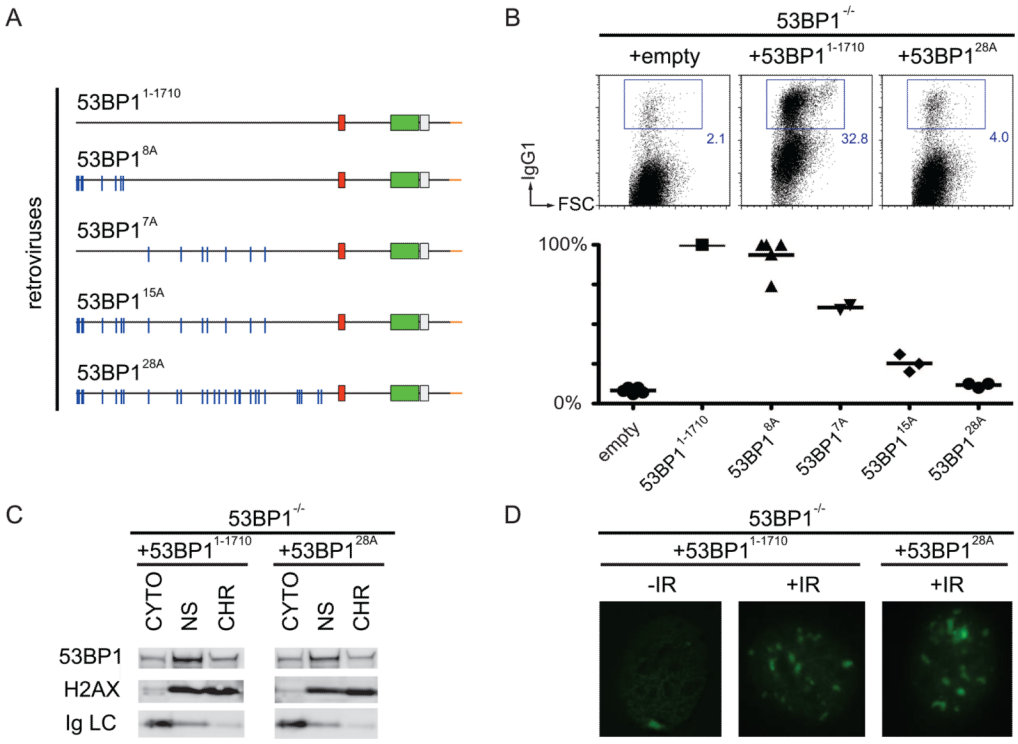

Figure 6. N-terminal phosphorylation of 53BP1 in DNA damage and CSR

(A) Diagram of 53BP1 retroviral constructs with the indicated mutations. **(B)** As in Figure 2(C) after infection of 53BP1$^{-/-}$ B cells with empty retrovirus, or retroviruses expressing 53BP1$^{1–1710}$, or the N-terminal mutant 53BP1^{28A}, or the other mutants listed in panel **(A).** **(C)** Western blots of fractionated 53BP1$^{-/-}$ B cells stimulated and infected with 53BP1$^{1–1710}$ or 53BP1^{28A}. **(D)** 53BP1 IRIF in 53BP1$^{-/-}$ MEFs reconstituted with 53BP1$^{1–1710}$ and 53BP1^{28A} after 10 Gy. See also Figure S5.

A

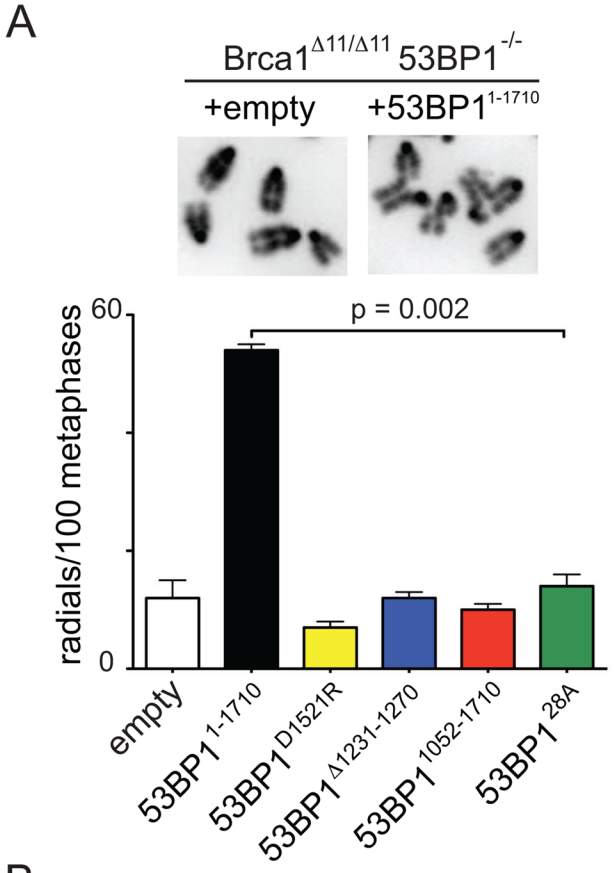

B

Domains of 53BP1	IR-foci	Chromatin binding	CSR	Resection
BRCT	D	D	D	D
Tudor (D1518/D1521)	R	R	R	R
Oligomerization	R	D	R	R
N-terminal Phosphorylations	D	D	R	R

D = dispensable R = required

Figure 7. Domains of 53BP1 required for preventing DNA end resection

(A) Brca1$^{\Delta 11/\Delta 11}$53BP1$^{-/-}$ B cells reconstituted with 53BP1 mutant retroviruses. Top: examples of normal metaphases (+empty) or metaphases containing radial chromosome structures (+53BP1$^{1-1710}$). Bottom: histogram quantitating the number of radial structures upon infection with the indicated retroviruses. **Error bars indicate standard error of the mean.** Two independent experiments. **(B)** Table summarizing which functional domains of 53BP1 are required (R) or dispensable (D) for IRIF, chromatin binding, CSR and protection of DNA ends from resection. See also Figure S6.